PHOTON LIMITED IMAGES AND THEIR RESTORATION

STANFORD UNIVERSITY

PREPARED FOR
ROME AIR DEVELOPMENT CENTER

MARCH 1976

RADC-TR-76-50
Technical Report
March 1976

PHOTON LIMITED IMAGES AND THEIR RESTORATION

Stanford University

Sponsored by
Defense Advanced Research Projects Agency
ARPA Order 2646

Rome Air Development Center
Air Force Systems Command
Griffiss Air Force Base, New York 13441

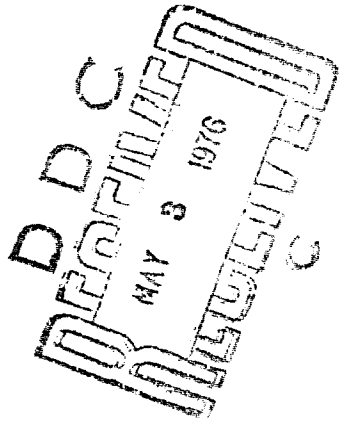

PHOTON LIMITED IMAGES AND THEIR RESTORATION

J. W. Goodman
J. F. Belsher

Contractor: Stanford University
Contract Number: F30602-75-C-0228
Effective Date of Contract: 1 April 1975
Contract Expiration Date: 31 May 1976
Amount of Contract: $40,000.00
Program Code Number: 6E20
Period of work covered: Apr 75 - Nov 75

Principal Investigator: Dr. Joseph W. Goodman
Phone: 415 497-3304

Project Engineer: Capt Edward C. Mahen, Jr.
Phone: 315 330-3145

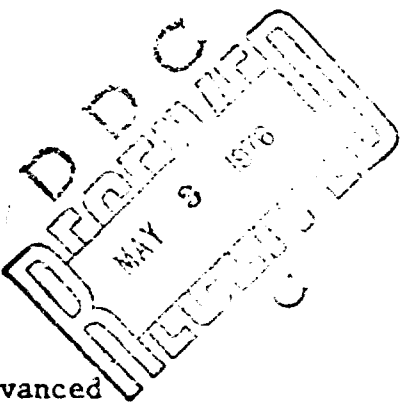

This research was supported by the Defense Advanced Research Projects Agency of the Department of Defense and was monitored by Capt Edward C. Mahen, Jr. (OCSF), Griffiss AFB NY 13441.

UNCLASSIFIED

SECURITY CLASSIFICATION OF THIS PAGE (When Data Entered)

REPORT DOCUMENTATION PAGE		READ INSTRUCTIONS BEFORE COMPLETING FORM
1. REPORT NUMBER RADC-TR-76-50	2. GOVT ACCESSION NO.	3. RECIPIENT'S CATALOG NUMBER
4. TITLE (and Subtitle) PHOTON LIMITED IMAGES AND THEIR RESTORATION		5. TYPE OF REPORT & PERIOD COVERED Interim Report 1 Apr 75 - 15 Nov 75 6. PERFORMING ORG. REPORT NUMBER N/A
7. AUTHOR(s) J. W. Goodman J. F. Belsher		8. CONTRACT OR GRANT NUMBER(s) F30602-75-C-0228
9. PERFORMING ORGANIZATION NAME AND ADDRESS Information Systems Laboratory Stanford Electronics Laboratories Stanford CA 94305		10. PROGRAM ELEMENT, PROJECT, TASK AREA & WORK UNIT NUMBERS 62301E 26460405
11. CONTROLLING OFFICE NAME AND ADDRESS Defense Advanced Research Projects Agency 1400 Wilson Blvd Arlington VA 22209		12. REPORT DATE March 1976 13. NUMBER OF PAGES 41
14. MONITORING AGENCY NAME & ADDRESS(if different from Controlling Office) Rome Air Development Center (OCSE) Griffiss AFB NY 13441		15. SECURITY CLASS. (of this report) UNCLASSIFIED 15a. DECLASSIFICATION/DOWNGRADING SCHEDULE N/A

16. DISTRIBUTION STATEMENT (of this Report)

Approved for public release; distribution unlimited.

17. DISTRIBUTION STATEMENT (of the abstract entered in Block 20, if different from Report)

Same

18. SUPPLEMENTARY NOTES

RADC Project Engineer: Capt Edward C. Mahen

Copies available in DDC.

19. KEY WORDS (Continue on reverse side if necessary and identify by block number)

Image Restoration
Photon limited Imaging

20. ABSTRACT (Continue on reverse side if necessary and identify by block number)

The prime practical limitation encountered in attempts to restore degraded imagery arises from noise inherent in the detected image data. In the first part of this report a model is developed which can be used to mathematically and statistically describe an image detected at low light levels. This model serves to clarify some basic properties of photon noise, and provides a basis for the analysis of image restoration. In the second part the problem of linear least-square restoration of imagery limited by photon noise is considered.

(Cont'd)

DD FORM 1 JAN 73 1473 EDITION OF 1 NOV 65 IS OBSOLETE

UNCLASSIFIED

SECURITY CLASSIFICATION OF THIS PAGE (When Data Entered)

The form of the invarient least-square restoration filter is derived using the statistical model appropriate for photon noise.

1. INTRODUCTION

The prime practical limitation encountered in attempts to restore degraded imagery arises from noise inherent in the detected image data. The most basic source of such noise lies in the photon fluctuations associated with the detection of the finite amount of light energy available to the imaging system. Thus photon fluctuations pose a fundamental limitation to the "restorability" of a degraded image.

In the first part of this report we develop a model which can be used to mathematically and statistically describe an image detected at low light levels. This model serves to clarify some of the basic properties of photon noise, and provides a basis for the analysis of image restoration to follow.

In the second part of the report we consider the problem of linear least-square restoration of imagery limited by photon noise. The form of the invariant least-square restoration filter is derived using the statistical model appropriate for photon noise. The mean-square error achievable with such a filter is then derived in terms of the total number of photo-events detected in the image, the complexity of the object, and the type and severity of the image blur. Finally, in the last part of the report, examples are presented for the case of atmospherically degraded images.

2. MODELING OF PHOTON-LIMITED IMAGERY

Our model for the detected imagery is essentially a two-dimensional analog of the semi-classical model developed by Mandel [1,2] for the study of photon counting statistics. This semi-classical model is known to yield results that are in complete agreement with a rigorous quantum

mechanical model for all detection problems involving the photoelectric effect [3]. Thus the vast majority of image detection problems are properly included in this framework.

2.1 SEMI-CLASSICAL MODEL

The model utilized is that of an inhomogeneous or compound Poisson impulse process. Thus the detected data $d(x,y)$ is represented by

$$d(x,y) = \sum_{n=1}^{N} \delta(x-x_n, y-y_n) \tag{1}$$

where $\delta(\cdot,\cdot)$ is a two-dimensional Dirac delta function, (x_n, y_n) represents the location of the n^{th} photoevent (i.e., the release of a photoelectron), and N is the total number of photoevents produced by the image. In this representation, N, x_n and y_n are all regarded as random variables, with statistical properties to be described in the following.

In accord with the semi-classical theory of photodetection, the probability that N events occur in an area A on the detector is taken to be Poisson,

$$P_A(N) = \frac{\left[\iint_A \lambda(x,y)\,dxdy\right]^N}{N!} \exp\left[-\iint_A \lambda(x,y)\,dxdy\right], \tag{2}$$

where the "rate" $\lambda(x,y)$ is related to the classical image intensity $i(x,y)$ falling on the detector through

$$\lambda(x,y) = \frac{\eta\, i(x,y)}{h\bar{\nu}}\,\tau \quad . \tag{3}$$

Here η is the quantum efficiency of the photosurface (assumed independent of (x,y)), h is Planck's constant, $\bar{\nu}$ is the mean optical frequency, and τ is the detector integration time.

Since the distribution $i(x,y)$ of classical intensity is unknown a priori, $\lambda(x,y)$ must ultimately be modeled as a random process. However, in calculating average properties of the detected image, it is often helpful to first treat $\lambda(x,y)$ as a given known function, and then average the results over the statistics of λ. This procedure is entirely consistent with Baye's rule of statistics. We further note for future use that, for a given $\lambda(x,y)$, the "event locations" (x_n,y_n) are independent random variables for different n's, with common probability density function [4]

$$p(x_n,y_n) = \frac{\lambda(x_n,y_n)}{\iint_{\infty}^{\infty} \lambda(x,y)\,dx\,dy} . \qquad (4)$$

Note further that, because $\lambda(x,y)$ is proportional to the classical intensity, $\lambda(x,y) \geq 0$.

Before turning to an examination of the image properties implied by this model, we point out some of the ways it can be generalized. First, in practice the photoevents registered by a real distributed detector consist of finite spatial pulses, not delta functions. This fact can be incorporated in our model by passing our ideal detected data (Eq.(1)) through a linear spatial filter, thus spreading the delta functions into pulses. Second, due to photoelectron multiplication noise, the areas and shapes of the various pulses may themselves be random variables. This property can be included in our model by making the spatial filter

randomly space-variant. These sophistications can all be included in the model, but since our interest lies in fundamental limits, there is little to be gained by incorporating these additional non-fundamental degradations.

We close this section by showing in Fig. 1 a typical classical intensity distribution and a corresponding typical detected image, the illustration being one-dimensional for simplicity.

2.2 SPECTRAL DENSITY OF PHOTON-LIMITED IMAGERY

One of the fundamental properties of a detected image is its spectral density. Our goal in this section is to calculate the spectral density of the detected image described by Eq.(1). If $D(\nu_X,\nu_Y)$ represents the Fourier transform of $d(x,y)$, i.e.,

$$D(\nu_X,\nu_Y) = \iint_{-\infty}^{\infty} d(x,y)e^{-j2\pi(\nu_X x+\nu_Y y)}dxdy \quad , \quad (5)$$

then our goal is to calculate

$$\Phi_d(\nu_X,\nu_Y) = E\left[|D(\nu_X,\nu_Y)|^2\right] \quad , \quad (6)$$

where the symbol $E[\cdot]$ indicates an expectation over the statistics of N, (x_n,y_n), and λ. Before making this calculation, we must first mention a physical restriction we impose on the random process $\lambda(x,y)$, i.e., on the statistical properties of the classical intensity in the image plane.

Any image produced by an optical system must contain finite total energy. From this fact it follows that for every sample function of the random process $\lambda(x,y)$,

$$\iint_{-\infty}^{\infty} \lambda(x,y)dxdy < \infty \quad . \quad (7)$$

This equation is sufficient to imply that any particular sample function $\lambda(x,y)$ has a well-defined Fourier transform,

$$\Lambda(\nu_X,\nu_Y) = \int\int_{-\infty}^{\infty} \lambda(x,y)e^{-j2\pi(\nu_X x+\nu_Y y)}dxdy \quad . \qquad (8)$$

Our goal now is to relate the spectral density $\Phi_d(\nu_X,\nu_Y)$ of the detected image to the spectral density

$$\Phi_\lambda(\nu_X,\nu_Y) = E\left[|\Lambda(\nu_X,\nu_Y)|^2\right] \qquad (9)$$

where the expectation is over the statistics of $\lambda(x,y)$.

To calculate the spectral density $\Phi_d(\nu_X,\nu_Y)$ of the detected image, we first Fourier transform Eq.(1), with the result

$$D(\nu_X,\nu_Y) = \sum_{n=1}^{N} e^{-j2\pi(\nu_X x_n+\nu_Y y_n)} \quad . \qquad (10)$$

The squared modulus of this quantity is

$$|D(\nu_X,\nu_Y)|^2 = \sum_{n=1}^{N}\sum_{m=1}^{N} e^{-j2\pi\left[\nu_X(x_n-x_m)+\nu_Y(y_n-y_m)\right]} \quad . \qquad (11)$$

It remains to find the expected value of this quantity over the statistics of N, (x_n,y_n) and $\lambda(x,y)$. It is convenient to first regard N and $\lambda(x,y)$ as given (known) quantities, average over the statistics of (x_n,y_n) and (x_m,y_m), and then average over N and λ. Thus our first goal is to compute

$$E_{nm}\left[|D(\nu_X,\nu_Y)|^2\right]$$

$$= \sum_{n=1}^{N}\sum_{m=1}^{N} E_{nm}\left[\exp\left\{-j2\pi\left[\nu_X(x_n-x_m)+\nu_Y(y_n-y_m)\right]\right\}\right] \qquad (12)$$

where E_{nm} signifies an average over (x_n,y_n) and (x_m,y_m).

Two classes of terms can be identified. First, there are N terms for which $n = m$, each of which yields unity. Second, there are $N^2 - N$ terms for which $n \neq m$. For such terms we know that (x_n,y_n) and (x_m,y_m) are independent random variables, and therefore that

$$p(x_n,y_n;x_m,y_m) = \frac{\lambda(x_n,y_n)}{\iint_{-\infty}^{\infty} \lambda(x,y)dxdy} \cdot \frac{\lambda(x_m,y_m)}{\iint_{-\infty}^{\infty} \lambda(x,y)dxdy} . \qquad (13)$$

For these $N^2 - N$ terms, the result of the averaging process is

$$E_{nm}\left[e^{-j2\pi\left[\nu_X(x_n-x_m)+\nu_Y(y_n-y_m)\right]}\right] = \left| \frac{\iint_{-\infty}^{\infty} \lambda(x,y)e^{-j2\pi(\nu_X x+\nu_Y y)}dxdy}{\iint_{-\infty}^{\infty} \lambda(x,y)dxdy} \right|^2 . \qquad (14)$$

The result of averaging $|D(\nu_X,\nu_Y)|^2$ over the statistics of (x_n,y_n) and (x_m,y_m) becomes

$$E_{nm}\left[|D(\nu_X,\nu_Y)|^2\right] = N + (N^2-N)\left|\frac{\Lambda(\nu_X,\nu_Y)}{\Lambda(0,0)}\right|^2 . \qquad (15)$$

Continuing our averaging process, we next find the expected value of Eq.(15) over the random variable N, given $\lambda(x,y)$. Representing the conditional mean of N (given λ) by $\bar{N}_{(\lambda)}$, and noting that, for Poisson statistics,

$$E\left[N^2-N\right] = \left(\bar{N}_{(\lambda)}\right)^2 \quad ,$$

$$\bar{N}_{(\lambda)} = \iint_{-\infty}^{\infty} \lambda(x,y)\,dxdy = \Lambda(0,0) \quad , \qquad (16)$$

we find that

$$E_{n,m,N}\left[\left|D(\nu_X,\nu_Y)\right|^2\right] = \bar{N}_{(\lambda)} + \left|\Lambda(\nu_x,\nu_y)\right|^2 \quad . \qquad (17)$$

Finally, averaging over the statistics of $\lambda(x,y)$, we obtain

$$\Phi_d(\nu_X,\nu_Y) = \bar{N} + \Phi_\lambda(\nu_X,\nu_Y) \qquad (18)$$

where $\bar{N}$ is the unconditional mean of N.

Thus the spectral density of the detected image is the sum of a constant spectral level $\bar{N}$, plus the spectral density of the rate function, Φ_λ. Alternate forms of this result are also useful. First, if we define a normalized spectral density

$$\hat{\Phi}_\lambda(\nu_X,\nu_Y) = \frac{\Phi_\lambda(\nu_X,\nu_Y)}{\Phi_\lambda(0,0)} \quad , \qquad (19)$$

then we have that

$$\Phi_d(\nu_X,\nu_Y) = \bar{N} + (\bar{N})^2\hat{\Phi}_\lambda(\nu_X,\nu_Y) \quad . \qquad (20)$$

Furthermore, since $\lambda(x,y)$ is proportional to the classical intensity $i(x,y)$, we must have

$$\hat{\Phi}_\lambda(\nu_X,\nu_Y) = \hat{\Phi}_i(\nu_X,\nu_Y) \qquad (21)$$

where $\hat{\Phi}_i(\nu_X,\nu_Y)$ is the spectral density of the classical intensity, normalized to unity at $\nu_X = \nu_Y = 0$. Thus we write our final result,

$$\Phi_d(\nu_X,\nu_Y) = \bar{N} + (\bar{N})^2\hat{\Phi}_i(\nu_X,\nu_Y) \quad . \qquad (22)$$

We illustrate this result in Fig. 2.

2.3 FLUCTUATIONS OF SPECTRAL DENSITY ESTIMATES

In a certain class of imaging problems, the desired end result is an accurate estimate of the normalized spectral density $\hat{\Phi}_i$ of the classical image intensity. For example, such is the case for Labeyrie's speckle interferometer [5], which is currently of great interest in astronomy. Because of the simple relation that exists between $\hat{\Phi}_i$ and the spectral density Φ_d of the detected image, a reasonable approach is to first estimate Φ_d, then express $\hat{\Phi}_i$ as (c.f. Eq.(22))

$$\hat{\Phi}_i = \frac{\Phi_d - \bar{N}}{(\bar{N})^2} \quad . \tag{23}$$

The quantity $\bar{N}$ is simply a measure of the total image brightness, which we assume is either known a priori or can be determined accurately by a suitable photometric measurement. Thus the fluctuations in our estimate of $\hat{\Phi}_i$ will be determined by the fluctuations inherent in our measurement of Φ_d. It is these fluctuations that we wish to find here.

An estimate of Φ_d is made by measuring $|D(\nu_x,\nu_y)|^2$ for a single detected image. The expected value of this measurement is, of course, $\Phi_d(\nu_x,\nu_y)$. But how far off from the expected value is a single measurement likely to be? To answer this question, we must find the second moment of $|D|^2$, i.e., we must calculate

$$E\left[|D|^4\right] = \sum_{n=1}^{N}\sum_{m=1}^{N}\sum_{p=1}^{N}\sum_{q=1}^{N} E\left[\exp\left\{-j2\pi\left[\nu_x(x_n-x_m+x_p-x_q)\right.\right.\right.$$

$$\left.\left.\left. + \nu_y(y_n-y_m+y_p-y_q)\right]\right\}\right] \quad . \tag{24}$$

This calculation is a lengthy one and is deferred to the Appendix. For a known (non-random) $\lambda(x,y)$, the result is

$$E\left[|D|^4\right] = \bar{N}_{(\lambda)} + 2\left(\bar{N}_{(\lambda)}\right)^2 + 4\left(1+\bar{N}_{(\lambda)}\right)|\Lambda(\nu_X,\nu_Y)|^2$$
$$+ |\Lambda(2\nu_X,2\nu_Y)|^2 \qquad (25)$$
$$+ \Lambda(2\nu_X,2\nu_Y)\left[\Lambda^*(\nu_X,\nu_Y)\right]^2 + \Lambda^*(2\nu_X,2\nu_Y)\left[\Lambda(\nu_X,\nu_Y)\right]^2$$
$$+ |\Lambda(\nu_X,\nu_Y)|^4 \quad .$$

Representing $\Lambda(\nu_X,\nu_Y)$ in terms of a modulus and phase,

$$\Lambda(\nu_X,\nu_Y) = |\Lambda(\nu_X,\nu_Y)|e^{j\theta(\nu_X,\nu_Y)} \qquad (26)$$

we can equivalently express the second moment of $|D|^2$ as

$$E\left[|D|^4\right] = \bar{N}_{(\lambda)} + 2\left(\bar{N}_{(\lambda)}\right)^2 + 4\left(1+\bar{N}_{(\lambda)}\right)|\Lambda(\nu_X,\nu_Y)|^2$$
$$+ |\Lambda(2\nu_X,2\nu_Y)|^2$$
$$+ 2|\Lambda(2\nu_X,2\nu_Y)||\Lambda(\nu_X,\nu_Y)|^2\cos\left[\theta(2\nu_X,2\nu_y) - 2\theta(\nu_X,\nu_Y)\right]$$
$$+ |\Lambda(\nu_X,\nu_Y)|^4 \quad . \qquad (27)$$

The task now remains of averaging over the statistics of $\lambda(x,y)$. If the image intensity distribution extends over a region of size $L\times L$, then under rather general conditions, the central limit theorem can be used to show that, for $\nu_X >> \frac{1}{L}$ and $\nu_Y >> \frac{1}{L}$, $\Lambda(\nu_X,\nu_Y)$ is approximately a circular complex gaussian random process, with correlation extending over a region of dimensions $\frac{2}{L}\times\frac{2}{L}$ in the frequency domain. It follows that the phase θ is uniformly distributed on $(-\pi,\pi)$, and that $|\Lambda|^2$ obeys negative exponential statistics. Furthermore, for such frequencies $\theta(2\nu_X,2\nu_X)$, $\theta(\nu_X,\nu_Y)$, $|\Lambda(2\nu_X,2\nu_Y)|$ and $|\Lambda(\nu_X,\nu_Y)|$ are all approximately independent. From these facts we conclude that

$$E\left[|\Lambda(\nu_X,\nu_Y)|^2\right] = \Phi_\lambda(\nu_X,\nu_Y)$$

$$E\left[|\Lambda(2\nu_X,2\nu_Y)|^2\right] = \Phi_\lambda(2\nu_X,2\nu_Y)$$

$$E\left[2|\Lambda(2\nu_X,2\nu_Y)||\Lambda(\nu_X,\nu_Y)|^2\cos\left[\theta(2\nu_X,2\nu_Y) - 2\theta(\nu_X,\nu_Y)\right]\right] = 0$$

$$E\left[|\Lambda(\nu_X,\nu_Y)|^4\right] = 2\Phi_\lambda^2(\nu_X,\nu_Y) \quad . \tag{28}$$

Now if we subtract the square of the mean of $|D|^2$, i.e., the square of Eq.(18), we obtain the variance of $|D|^2$,

$$\sigma^2_{|D|^2} = \bar{N} + (\bar{N})^2 + 2(2+\bar{N})\Phi_\lambda(\nu_X,\nu_Y) + \Phi_\lambda(2\nu_X,2\nu_Y) + \Phi_\lambda^2(\nu_X,\nu_Y) \quad . \tag{29}$$

Equivalently, using (21), we have

$$\sigma^2_{|D|^2} = \bar{N} + (\bar{N})^2 + 2(2+\bar{N})(\bar{N})^2\hat{\Phi}_i(\nu_X,\nu_Y) + (\bar{N})^2\hat{\Phi}_i(2\nu_X,2\nu_Y) + (\bar{N})^2\hat{\Phi}_i^2(\nu_X,\nu_Y) \quad . \tag{30}$$

An important conclusion can be drawn directly from Eq.(30). The fluctuations of the spectral density of the detected image at frequency (ν_X,ν_Y) depend not only on the spectral density of the classical intensity at (ν_X,ν_Y), but also on that spectral density at frequency $(2\nu_X,2\nu_Y)$! Stated in other words, a frequency component of the classical intensity at frequency $(2\nu_X,2\nu_Y)$ induces fluctuations of the spectrum at (ν_X,ν_Y). This "half-frequency noise" phenomenon is a fundamental property of photon limited images. It has been noted previously in a different but related context by Walkup [6].

We close this section by presenting an expression for the rms signal-to-noise ratio associated with an estimate of $\hat{\Phi}_i$ at frequency (ν_X,ν_Y). Subtracting the bias $\bar{N}$ associated with the mean of $|D|^2$,

we obtain

$$\left(\frac{S}{N}\right)_{rms} = \frac{E\left[|D|^2\right] - \bar{N}}{\sigma_{|D|^2}} \tag{31}$$

$$= \frac{\hat{\phi}_i(\nu_X,\nu_Y)}{\left[\hat{\phi}_i^2(\nu_X,\nu_Y) + \frac{2}{\bar{N}}\hat{\phi}_i(\nu_X,\nu_Y) + \frac{1}{(\bar{N})^2}\left[1+4\hat{\phi}_i(\nu_X,\nu_Y)+\hat{\phi}_i(2\nu_X,2\nu_Y)\right] + \frac{1}{(\bar{N})^3}\right]^{\frac{1}{2}}} .$$

Note that as $\bar{N} \to \infty$, the r.m.s. signal-to-noise ratio approaches unity, in agreement with the classical results on the statistical fluctuations of periodograms [7].

Figure 3 illustrates the conclusions of this analysis with a specific example. The classical intensity distribution is taken to be a sinusoidal fringe of frequency ν_0 and length L. A typical sample function of $|D(\nu)|^2$ is shown. Note that excess fluctuations are present at $\nu_0/2$ due to the presence of the fringe at frequency ν_0.

3. LINEAR LEAST-SQUARES RESTORATION OF DEGRADED PHOTON-LIMITED IMAGES

In many practical problems of interest, the detected image data arises from a blurred image of the object of interest. For example, the object may suffer significant motion during the detection interval , thus blurring the image. Alternatively, and of greater interest here, the detected image may be seriously degraded by the spatial and temporal fluctuations of the refractive index of the atmosphere, i.e., by "atmospheric seeing". At low light levels, the detected image further suffers from photon noise of the type discussed in the previous section. In order to extract as much information as possible about the object from the detected image data, we seek a method of image restoration which will enhance object

detail without unduly emphasizing the noise associated with the discrete photo-events composing the detected image. In the sections to follow, we consider one approach to this problem.

3.1 LINEAR LEAST-SQUARES RESTORATION

The approach we shall investigate here is commonly referred to as linear least-squares restoration. The philosophy behind this approach is perhaps best explained with the aid of Fig. 4. The function $o(x,y)$ represents the true object brightness distribution, or alternatively the image that would be produced by an ideal optical system (free from aberrations and free from any blur due to diffraction) and an ideal noise-free detector. Our goal is to determine $o(x,y)$ from the actual detected data with the greatest possible accuracy. Following the upper branch of Fig. 4, the ideal object suffers a perfectly known blur on passage to the image plane, this blur being introduced by diffraction, fixed aberrations, and other external causes, such as object motion, atmospheric seeing, etc. We assume that all of these blurs can be lumped together and represented by a single known linear, space-invariant filter, with impulse response $b(x,y)$, or optical transfer function $\hat{B}(\nu_x,\nu_y)$,

$$\hat{B}(\nu_x,\nu_y) = \frac{\displaystyle\int_{-\infty}^{\infty}\!\!\int b(x,y)e^{-j2\pi(\nu_x x+\nu_y y)}\,dxdy}{\displaystyle\int_{-\infty}^{\infty}\!\!\int b(x,y)\,dxdy} \quad . \tag{32}$$

To represent the statistical fluctuations introduced by the detection process, the blurred image is now applied to a "Poisson generator", which produces a Poisson impulse process with rate $\lambda(x,y)$ proportional to the intensity of the blurred image. The output of the Poisson generator is

the detected image data $d(x,y)$, on which we must base our estimate of $o(x,y)$.

Our restoration procedure is to apply the detected image data to a linear, space-invariant restoration filter with impulse response $h(x,y)$ and optical transfer function $\hat{H}(\nu_x,\nu_y)$. This transfer function will be chosen to minimize the expected value of the mean-squared error,

$$E\left[\int_{-\infty}^{\infty} e^2(x,y)dxdy\right] = E\left[\int_{-\infty}^{\infty} |r(x,y)-o(x,y)|^2 dxdy\right], \tag{33}$$

where the error $e(x,y)$ represents the difference between the restored image $r(x,y)$ and a certain filtered version of the object, $o(x,y)$, the expectation being over the statistics of $o(x,y)$ and the statistics of the detection process.

The choice of a filtered object $\tilde{o}(x,y)$, rather than the true object $o(x,y)$, for defining the error requires some comment. The restoration of object frequency components beyond the diffraction-limited cutoff of the optical system is impossible to achieve with any linear invariant restoration filter. Hence the best we can hope to accomplish is restoration of those frequency components lying within the diffraction-limited passband. Accordingly, we count as error only the differences between the restored spectrum $R(\nu_x,\nu_y)$ and the (possibly modified) portion of the spectrum lying within the observable passband. The frequency spectrum of $\tilde{o}(x,y)$ is thus

$$\tilde{O}(\nu_x,\nu_y) = \begin{cases} O(\nu_x,\nu_y)\hat{S}(\nu_x,\nu_y) & (\nu_x,\nu_y) \text{ in observable passband} \\ 0 & \text{otherwise} \end{cases} \tag{34}$$

Usually we will take $\hat{S}(\nu_x, \nu_y)$ to be of the form

$$\hat{S}(\nu_x, \nu_y) = \begin{cases} 1 & (\nu_x, \nu_y) \text{ in observable passband} \\ 0 & \text{otherwise} \end{cases} \quad (35)$$

However, we note that the resulting $\tilde{o}(x,y)$ can have negative values in this case. We could alternatively choose $\hat{S}(\nu_x, \nu_y)$ to be the diffractic limited optical transfer function of the system, thus guaranteeing a positive $\ddot{o}(x,y)$. In the analysis to follow we leave $\hat{S}(\nu_x, \nu_y)$ completely general, but eventually we choose the form of Eq.(35) for mathematical simplicity.

Some final comments are in order regarding the non-optimality of the restoration procedure described above. First, it is well known that linear least-squares restoration is not optimal in the sense of maximum likelihood or maximum a posteriori probability when the image statistics are Poisson. Rather, non-linear filtering is required for true optimality [7]. Secondly, the choice of a space-invariant linear restoration filter undoubtedly reduces performance even further; it seems clear intuitively that a space-variant filter can perform better than a space-invariant filter in the presence of signal-dependent noise. However, it should be pointed out that both optimal non-linear filtering and optimal space-variant linear filtering are in general computationally less efficient than linear space-invariant filtering. For this reason, there remains a strong interest in knowing the limitations of linear space-invariant least-squares restoration for photon-limited imagery.

3.2 THE FORM OF THE RESTORATION FILTER AND THE QUALITY OF THE RESTORED IMAGE

In this section we first derive the form of the linear space-invariant least-square restoration filter for photon-limited images. Our goal is to choose a filter transfer function H which minimizes $E\left[\int\int_{-\infty}^{\infty} e^2(x,y)dxdy\right]$. By Parseval's theorem, it is equivalent to minimize $E\left[\int\int_{-\infty}^{\infty} |\mathcal{E}(\nu_X,\nu_Y)|^2 d\nu_X,d\nu_Y\right]$, where $\mathcal{E}$ is the Fourier transform of e. Interchanging orders of integration and expectation, we find that it suffices to minimize at each (ν_X,ν_Y)

$$E\left[|\mathcal{E}(\nu_X,\nu_Y)|^2\right] = E\left[|DH - O|^2\right] \tag{36}$$

where $O(\nu_X,\nu_Y)$ is the Fourier transform of $o(x,y)$. The minimization is straightforward and yields

$$H(\nu_X,\nu_Y) = \frac{\Phi^*_{do}}{\Phi_d} \tag{37}$$

where Φ_d is the spectral density of the detected image $d(x,y)$, while $\Phi_{d\tilde{o}}$ is the cross-spectral density of $d(x,y)$ and $o(x,y)$,

$$\Phi_{do}(\nu_X,\nu_Y) = E\left[D(\nu_X,\nu_Y)O^*(\nu_X,\nu_Y)\right] . \tag{38}$$

Straightforward calculations, using the Poisson impulse model, show that

$$\begin{aligned}\Phi_d(\nu_X,\nu_Y) &= \bar{N} + (\bar{N})^2|\hat{B}(\nu_X,\nu_Y)|^2\Phi_o(\nu_X,\nu_Y)\\ \Phi^*_{do}(\nu_X,\nu_Y) &= (\bar{N})^2\hat{S}(\nu_X,\nu_Y)B^*(\nu_X,\nu_Y)\Phi_o(\nu_X,\nu_Y) .\end{aligned} \tag{39}$$

We conclude that the transfer function of the restoration filter is given by

$$H(\nu_X,\nu_Y) = \frac{\bar{N}\,\hat{S}(\nu_X,\nu_Y)\hat{B}^*(\nu_X,\nu_Y)\hat{\phi}_o(\nu_X,\nu_Y)}{1+\bar{N}|\hat{B}(\nu_X,\nu_Y)|^2\hat{\phi}_o(\nu_X,\nu_Y)} \quad . \tag{40}$$

Note that at zero spatial frequency the gain of this filter is $\bar{N}/(1+\bar{N})$. Thus the normalized restoration transfer function is

$$\hat{H}(\nu_X,\nu_Y) = \frac{(1+\bar{N})\hat{S}(\nu_X,\nu_Y)\hat{B}^*(\nu_X,\nu_Y)\hat{\phi}_o(\nu_X,\nu_Y)}{1+\bar{N}|\hat{B}(\nu_X,\nu_Y)|^2\hat{\phi}_o(\nu_X,\nu_Y)} \quad . \tag{41}$$

We turn next to calculation of the total mean-squared error ε achieved when the restoration filter of Eq.(40) is used. Using (36) we see that

$$\begin{aligned}\varepsilon &= E\left[\int_{-\infty}^{\infty}\int |\mathcal{E}(\nu_Y,\nu_Y)|^2 d\nu_X\, d\nu_Y\right] \\ &= \int_{-\infty}^{\infty}\int\left[|H|^2\phi_d - H\phi_{d\tilde{o}} - H^*\phi^*_{d\tilde{o}} + \phi_{\tilde{o}}\right]d\nu_X\, d\nu_Y \quad .\end{aligned} \tag{42}$$

Substituting (39) and (40) in (42), we obtain after some algebra

$$\varepsilon = \int_{-\infty}^{\infty}\int \frac{(\bar{N})^2|\hat{S}|^2\hat{\phi}_o}{1+\bar{N}|\hat{B}|^2\hat{\phi}_o}\, d\nu_X\, d\nu_Y \quad . \tag{43}$$

The total mean-square error in the image is not a particularly meaningful quantity in itself. Note in particular that, as $\bar{N}$ grows large, so too does ε, in direct proportion to $\bar{N}$. However, the mean-square value of the object within the observable passband is $(\bar{N})^2\int_{-\infty}^{\infty}\int|\hat{S}|^2\hat{\phi}_o d\nu_X d\nu_Y$; hence the "signal" component of the output power rises in proportion to $(\bar{N})^2$, yielding a net increase in restored image quality as $\bar{N}$ increases.

It is highly appealing to define a single parameter Q to represent the overall quality of the restored image. Many definitions of such a parameter are possible, but none can be fully justified as being the best conceivable choice. Here we shall consider two possible choices for a definition of Q.

Our first definition depends on the mean-square error ε, which takes into account both the statistical fluctuations of the restored image due to the photodetection process and the defects of the restored image caused by residual uncompensated blur. Noting that as $\bar{N} \to 0$, $\varepsilon \to (\bar{N})^2 \iint_{-\infty}^{\infty} |S|^2 \hat{\Phi}_o d\nu_x d\nu_y$, we find the proper definition of the quality factor to be

$$Q_1 = \frac{(\bar{N})^2 \iint_{-\infty}^{\infty} |\hat{S}|^2 \hat{\Phi}_o d\nu_x d\nu_y}{\varepsilon} - 1 ,$$

or equivalently

$$Q_1 = \frac{\iint_{-\infty}^{\infty} |\hat{S}|^2 \hat{\Phi}_o d\nu_x d\nu_y}{\iint_{\infty}^{\infty} \frac{|\hat{S}|^2 \hat{\Phi}_o d\nu_x d\nu_y}{1 + \bar{N}|\hat{B}|^2 \hat{\Phi}_o}} - 1 . \tag{44}$$

A second possible quality parameter which has a great deal of appeal will now be discussed. This second parameter is defined to be

$$Q_2 = (\Delta\nu)^2 \log\left(1 + \frac{S}{N}\right) \tag{45}$$

where $(\Delta\nu)^2$ is a measure of the two-dimensional restored bandwidth, while S/N is a measure of the mean-square signal-to-noise ratio in the restored image. The similarity of this quality measure to a measure of information content is apparent. A reasonable definition of the restored

bandwidth is

$$(\Delta\nu)^2 = \iint_{-\infty}^{\infty} |\hat{\hat{B}}\hat{\hat{H}}| d\nu_X d\nu_Y \tag{46}$$

where

$$\hat{\hat{B}}\hat{\hat{H}} = \frac{(1+\bar{N})\hat{S}(\nu_X,\nu_Y)|\hat{B}(\nu_X,\nu_Y)|^2\hat{\Phi}_o(\nu_X,\nu_Y)}{1 + \bar{N}|\hat{B}(\nu_X,\nu_Y)|^2\hat{\Phi}_o(\nu_X,\nu_Y)} . \tag{47}$$

As for the parameter S/N , the choice of a definition is less clear cut. One suitable choice is the mean-square signal-to-noise ratio <u>per degree of freedom of the restored image</u>,

$$\frac{S}{N} = \frac{\bar{N}}{A_i(\Delta\nu)^2} \tag{48}$$

where A_i represents the area occupied by the restored image. Only the first of the above quality measures (Q_1) will be used in section 4.

3.3 THE DEPENDENCE OF THE NORMALIZED SPECTRAL DENSITY OF THE OBJECT ON OBJECT COMPLEXITY

The results of the previous sections have demonstrated that the degree to which restoration is possible depends not only on the total light flux ($\bar{N}$) and the optical transfer function of the blur ($\hat{B}$), but also on the normalized spectral density of the object ($\hat{\Phi}_o$). In this section we explore the dependence of this normalized spectrum on "object complexity". To explore this question in a completely general way is extremely difficult. Accordingly, we examine two specific models of the object, neither of which is entirely realistic, but from which we can deduce trends valid for more general object models.

For comparison purposes we note that the simplest possible object is an ideal point source, with brightness distribution

$$o(x,y) = o_o \delta(x-x_1, y-y_1) \quad . \tag{49}$$

While such an object cannot exist physically, nonetheless it serves as a useful idealized case against which we can compare the results of complicated object models. For the point source described above, the normalized spectral density is given by

$$\Phi_o(\nu_x, \nu_y) = 1 \qquad (\text{all } \nu_x, \nu_y) \quad . \tag{50}$$

The first model utilized to represent a more complicated object is a natural generalization of the case of a single point source. We suppose that there exist M equally intense point sources,

$$o(x,y) = \sum_{m=1}^{M} o_o \delta(x-x_m, y-y_m) \quad . \tag{51}$$

We suppose that the locations (x_m, y_m) are independent random variables, uniformly distributed over a square object field of size $L \times L$. Omitting the calculations, which are straightforward, we find the normalized object spectral density in this case to be

$$\Phi_o(\nu_x, \nu_y) = \frac{1}{M} + \left(1 - \frac{1}{M}\right) \text{sinc}^2 L\nu_x \, \text{sinc}^2 L\nu_y \tag{52}$$

which is shown in Fig. 5a. Note that an increase of object complexity has led to a decrease in the level of the normalized spectral density, except at extremely low spatial frequencies.

What is the effect of object complexity, represented by M, on the quality of the restored image? Using the fact that $\Phi_o \approx \frac{1}{M}$ over most spatial frequencies of interest, examination of Eqs. (44), (45)

and (48) shows that Q_1 and Q_2 are primarily functions of the total number of photoevents contributed by a single point source,

$$\bar{n} = \frac{\bar{N}}{M} \quad . \tag{53}$$

If $\bar{n}$ is held fixed, Q is essentially independent of how many point sources are in the field.

A second and somewhat more general model for the object can be formulated as follows. Let the object be modeled as a stationary random process, $o(x,y) \geq 0$, with mean $\bar{o} > 0$ and variance σ_o^2. We further suppose that this stationary random process is confined to an $L \cdot L$ square, and is zero outside that square. This space limitation can be explicitly introduced by multiplying the stationary $o(x,y)$ by a window function $\mathrm{rect}(x/L)\mathrm{rect}(y/L)$. We wish to calculate the normalized spectral density for this object model. The calculation is tedious but again straightforward. To state the results in succinct form, we define the following additional symbols:

$A = L^2$ represents the area of the object field;

A_c represents the correlation area of the random process $o(x,y)$, and is specifically defined as

$$A_c = \iint_{-\infty}^{\infty} \gamma_o(\Delta x, \Delta y)\, d\Delta x\, d\Delta y$$

where γ_o is the autocovariance of $o(x,y)$, normalized to unity at the origin; and

$\Phi_{\delta o}(\nu_x, \nu_y)$ is the spectral density of the fluctuations of the object about its mean, normalized to unity at the origin.

With these definitions, the normalized spectral density can be expressed approximately as

$$\hat{\Phi}_o(\nu_x,\nu_y) \doteq \left[1 - \left(\frac{\sigma_o}{\bar{o}}\right)^2 \frac{A_c}{A}\right] \mathrm{sinc}^2 L\nu_x \; \mathrm{sinc}^2 L\nu_y + \left(\frac{\sigma_o}{\bar{o}}\right)^2 \frac{A_c}{A} \; \hat{\Phi}_{\delta o}(\nu_x,\nu_y) \tag{54}$$

where the chief approximation is that

$$\left(\frac{\sigma_o}{\bar{o}}\right)^2 \frac{A_c}{A} \ll 1 \quad . \tag{55}$$

Figure 5b shows a typical plot of this normalized spectral density. Of most importance, we note that, except at the lowest spatial frequencies, the normalized spectral density has a value less than $(\sigma_o/\bar{o})^2(A_c/A)$. This parameter plays a role similar to $(M)^{-1}$ in the previous model. In this case we define the parameter $\bar{n}$ as the mean number of photoevents contributed by a single correlation area of the object.

$$\bar{n} = \frac{\bar{N}}{A} \cdot A_c \tag{56}$$

Again referring to Eqs.(44), (45) and (48), we find that the quality of the restored image will depend primarily on the parameter $\bar{n}(\sigma_o/\bar{o})^2$ for any given blur.

4. APPLICATION TO ATMOSPHERICALLY DEGRADED IMAGES

Our goal here is to apply the results of section 3 to the specific case of atmospherically degraded images. All imagery considered here will be assumed to be recorded with an exposure time that is much longer than the characteristic fluctuation time of the atmosphere. Thus we are

dealing only with long-exposure imagery. However, we consider both ordinary long-exposure imagery and "tilt-removed" long-exposure imagery. In the second case it is assumed that a perfect tilt removal system operates to keep the image perfectly centered on a fixed point at all times.

Using the results of Fried [8], we have that the OTF of atmospherically induced blur is given by

$$\hat{B}_A(\nu) = \exp\left\{-3.44\left(\frac{\bar{\lambda}\nu F}{r_o}\right)^{5/3}\left[1 - \alpha\left(\frac{\bar{\lambda}\nu F}{D}\right)^{1/3}\right]\right\} \qquad (57)$$

where

$\bar{\lambda}$ is the mean wavelength;

F is the focal length of the telescope;

D represents the telescope diameter;

$\nu = \sqrt{\nu_x^2 + \nu_y^2}$ represents radius in the spatial frequency plane;

r_o represents the coherence parameter of the atmospheric wavefront distortions, as defined by Fried [8]; and

α takes on the value zero, one half, or one, according to whether the image is recorded with no tilt removal ($\alpha=0$); with tilt removal and "far field" atmospheric propagation conditions [8] ($\alpha=\frac{1}{2}$); or with tilt removal and "near field" atmospheric propagation conditions [8] ($\alpha=1$).

In addition to the atmospherically induced blur, we assume that blur is introduced due to diffraction by the finite aperture size of the telescope. For a perfect circular telescope, we have an optical transfer function

$$\hat{B}_T(\nu) = \frac{2}{\pi}\left[\cos^{-1}\left(\frac{\nu}{\nu_o}\right) - \frac{\nu}{\nu_o}\sqrt{1 - \left(\frac{\nu}{\nu_o}\right)^2}\right] \tag{58}$$

for $\nu \leq \nu_o$, zero otherwise, where $\nu_o = D/(\bar{\lambda}F)$ represents the diffraction limited cutoff frequency. For computational purposes, a convenient approximation due to Hufnagel [9] can be used,

$$\hat{B}_T(\nu) \tilde{=} 1 - 1.25\left(\frac{\nu}{\nu_o}\right) + 0.25\left(\frac{\nu}{\nu_o}\right)^4 . \tag{59}$$

The total OTF of the imaging system is simply the product of Eqs.(57) and (58) or (59),

$$\hat{B}(\nu) = \hat{B}_T(\nu)\hat{B}_A(\nu) \quad . \tag{60}$$

Incorporating the definition of ν_o in Eq.(57), we obtain for the total OTF,

$$\hat{B}(\nu) \tilde{=} \left[1 - 1.25\left(\frac{\nu}{\nu_o}\right) + 0.25\left(\frac{\nu}{\nu_o}\right)^4\right] \times \exp\left\{-3.44\left(\frac{\nu}{\nu_o}\right)^{5/3}\left(\frac{D}{r_o}\right)^{5/3}\left[1 - \alpha\left(\frac{\nu}{\nu_o}\right)^{1/3}\right]\right\} \tag{61}$$

for $\nu \leq \nu_o$, zero otherwise.

We have used numerical integration to calculate $(\Delta\nu)^2$ (Eq.(46)), and Q_1 (Eq.(44)) for the case of a point-source object ($\hat{\phi}_o = 1$) with blur $\hat{B}$ of Eq.(61), and an ideal transfer function $\hat{S}$ of Eq.(35). In this case,

$$(\Delta\nu)^2 = 2\pi(1+\bar{N}) \int_0^{\nu_o} \frac{|\hat{B}(\nu)|^2 \nu \, d\nu}{1 + \bar{N}|\hat{B}(\nu)|^2} \tag{62}$$

and we can show

$$Q_1 = \frac{(\Delta\nu)^2}{\pi\nu_o^2 - (\Delta\nu)^2} \quad . \tag{63}$$

In the computations we have assumed the parameter values

$$r_o = 10 \text{ cm and } 5 \text{ cm}$$

$$D = 152.5 \text{ cm}$$

$$\bar{\lambda} = 5\times10^{-5} \text{ cm} \quad .$$

It is not necessary to assume a specific focal length for the telescope if we work with spatial frequencies $\Omega = F\nu$ measured in cycles per radian of arc in the sky. The ratio of ν/ν_o in Eq.(61) is replaced by Ω/Ω_o, where $\Omega_o = F\nu_o$, and we calculate $(\Delta\Omega)^2 = F^2(\Delta\nu)^2$ rather than $(\Delta\nu)^2$. Likewise, Q_1 is re-defined as

$$Q_1 = \frac{(\Delta\Omega)^2}{\pi\Omega_o^2 - (\Delta\Omega)^2} \quad , \tag{64}$$

with no change in its numerical values resulting.

In Fig. 6 we show plots of the "maximum restorable frequency" $\Delta\Omega/\sqrt{\pi}$ vs. $\bar{N}$ for the case of a point-source object and the parameter values specified above. The incident light flux is varied over eight orders of magnitude. Figure 6a corresponds to the "no tilt removal" case, while 6b and 6c represent the "tilt removed" cases for far-field and near-field atmospheric propagation conditions, respectively. Note that in all cases, the maximum restorable frequency increases very slowly with $\bar{N}$, implying that, for the parameter values specified here, truly enormous amounts of light flux are necessary to record an image which can be substantially restored.

To illustrate this point further, consider the transfer function $\hat{B}\hat{H}$ of the cascade of the blur and the deblur. From Eq.(47) with

$\bar{N} >> 1$ and $\hat{\phi}_o = 1$, we see that within the diffraction-limited passband we have

$$\hat{B}\hat{H} = \frac{\bar{N}|\hat{B}|^2}{1 + \bar{N}|\hat{B}|^2} \tag{65}$$

If we wish to restore the frequency component at ν to ½ the amplitude it had before the blur, we require that $\bar{N}|\hat{B}|^2 = 1$, or

$$\bar{N} = |\hat{B}|^{-2} \quad . \tag{66}$$

Assuming that $\alpha = 0$ (no tilt removal) and for simplicity neglecting the diffraction-limited portion of the OTF, we require from Eq.(61) that

$$\bar{N} = \exp\left\{6.88\left(\frac{\Omega}{\Omega_o}\right)^{5/3}\left(\frac{D}{r_o}\right)^{5/3}\right\} \quad . \tag{67}$$

With $D = 152$ cm, $r_o = 10$ cm and $\bar{\lambda} = 5\times10^{-5}$ cm, we find

$$\bar{N} = \exp\left\{6.88\left(\frac{\Omega}{200}\right)^{5/3}\right\}$$

with Ω expressed in cycles per milliradian. Now for $\Omega = \Omega_o/2 = 1520$ cycles per milliradian, we find that

$$\bar{N} \simeq 6\times10^{87} \text{ photoevents} .$$

Thus more than 10^{87} photoevents are required in the detection process to achieve this degree of restoration!

In Fig. 7 we have plotted the quality factor Q_1 for the same range of $\bar{N}$, again for two values of r_o. Figures 7a, b and c

again correspond to no tilt removal, tilt removed with far-field atmospheric propagation, and tilt removed with near-field atmospheric propagation. Again, for the parameters chosen, there is only a small change of image quality over this wide range of $\bar{N}$.

These results support the experimentally observed fact that long-time-average atmospherically degraded images are extremely difficult to restore in practice. In principle, if enough light flux were utilized in the detection of the image, significant restoration would be possible However, the theoretical results above imply that, for the conditions of interest here, the amount of light flux required is prohibitively large.

We note in closing that, although the results above have been derived for the case of a point-source object, they can be shown to be a close approximation for the case of a more complicated object provided $\sigma_o/\bar{o} \approx 1$ and $\bar{N}$ is replaced by $\bar{n}$, the average number of photoevents per correlation area of the object.

5. FUTURE WORK

The formalism described above is now ready for application to several problems important for compensated imaging. We are now in the process of deriving comparable results for the case of a partially compensated imaging system, modeling the residual wavefront errors as a gaussian phase screen. In addition, we intend to explore the restorability of short-exposure images using the model developed here.

APPENDIX

Our goal in this appendix is to show that the fourth-order moment of Eq.(24) reduces to the result indicated in Eq.(25). Thus we wish to find

$$E\left[|D_i|^4\right] = \sum_{n=1}^{N}\sum_{m=1}^{N}\sum_{p=1}^{N}\sum_{q=1}^{N} E\left[\exp\left\{-j2\pi\left[\nu_X(x_n-x_m+x_p-x_q) + \nu_Y(y_n-y_m+y_p-y_q)\right]\right\}\right] \quad . \tag{A-1}$$

The N^4 terms in this summation can be placed in 15 different classes as follows:

(1)	n=m=p=q	N terms
(2)	n=m, p=q, n≠p	N(N-1) terms
(3)	n=m, p≠q≠n	N(N-1)(N-2) terms
(4)	n=p, m=q, n≠m	N(N-1) terms
(5)	n=p, m≠q≠n	N(N-1)(N-2) terms
(6)	n=q, m=p, n≠m	N(N-1) terms
(7)	n=q, m≠p≠n	N(N-1)(N-2) terms
(8)	n=m=p, n≠q	N(N-1) terms
(9)	n=m=q, n≠p	N(N-1) terms
(10)	n=p=q, n≠m	N(N-1) terms
(11)	p=q=m, n≠m	N(N-1) terms
(12)	n≠m≠p≠q	N(N-1)(N-2)(N-3) terms
(13)	p=q, n≠m≠p	N(N-1)(N-2) terms
(14)	m=q, n≠m≠p	N(N-1)(N-2) terms
(15)	m=p, n≠m≠q	N(N-1)(N-2) terms

We regard the rate $\lambda(x,y)$ of the process as a known, deterministic function, and average over the $2N+1$ random variables (x_1,y_1), (x_2,y_2), ... (x_N,y_N), N. Noting that, for a Poisson random variable N,

$$E_N\left[N(N-1 \ldots (N-k+1)\right] = \left[\overline{N}_{(\lambda)}\right]^k , \qquad (A-2)$$

the contributions of the 15 sets of terms are:

(1) $\overline{N}_{(\lambda)}$

(2) $\left[\overline{N}_{(\lambda)}\right]^2$

(3) $\left[\overline{N}_{(\lambda)}\right]^3 |\hat{\Lambda}(\nu_X,\nu_Y)|^2$

(4) $\left[\overline{N}_{(\lambda)}\right]^2 |\hat{\Lambda}(2\nu_X,2\nu_Y)|^2$

(5) $\left[\overline{N}_{(\lambda)}\right]^3 \hat{\Lambda}(2\nu_X,2\nu_Y)\left[\hat{\Lambda}^*(\nu_X,\nu_Y)\right]^2$

(6) $\left[\overline{N}_{(\lambda)}\right]^2$

(7) $\left[\overline{N}_{(\lambda)}\right]^3 |\hat{\Lambda}(\nu_X,\nu_Y)|^2$

(8) $\left[\overline{N}_{(\lambda)}\right]^2 |\hat{\Lambda}(\nu_X,\nu_Y)|^2$

(9) $\left[\overline{N}_{(\lambda)}\right]^2 |\hat{\Lambda}(\nu_X,\nu_Y)|^2$

(10) $\left[\overline{N}_{(\lambda)}\right]^2 |\hat{\Lambda}(\nu_X,\nu_Y)|^2$

(11) $\left[\overline{N}_{(\lambda)}\right]^2 |\hat{\Lambda}(\nu_X,\nu_Y)|^2$

(12) $\left[\overline{N}_{(\lambda)}\right]^4 |\hat{\Lambda}(\nu_X,\nu_Y)|^4$

(13) $\left[\overline{N}_{(\lambda)}\right]^3 |\hat{\Lambda}(\nu_X,\nu_Y)|^2$

(14) $\left[\overline{N}_{(\lambda)}\right]^3 \hat{\Lambda}^*(2\nu_X,2\nu_Y)\left[\hat{\Lambda}(\nu_X,\nu_Y)\right]^2$

(15) $\left[\overline{N}_{(\lambda)}\right]^3 |\hat{\Lambda}(\nu_X,\nu_Y)|^2$.

Here, as before, the definition

$$\hat{\Lambda}(\nu_X,\nu_Y) = \frac{\iint_{-\infty}^{\infty} \lambda(x,y)\, e^{-j2\pi(\nu_X x+\nu_Y y)}\, dxdy}{\iint_{\infty}^{\infty} \lambda(x,y)\, dxdy} \qquad \text{(A-3)}$$

is used. Noting further that

$$\Lambda(\nu_X,\nu_Y) = \bar{N}_{(\lambda)}\hat{\Lambda}(\nu_X,\nu_Y) \quad , \qquad \text{(A-4)}$$

and combining all of these results, we obtain Eq.(25),

$$\begin{aligned} E\left[|D|^4\right] &= \bar{N}_{(\lambda)} + 2\left(\bar{N}_{(\lambda)}\right)^2 + 4\left(1+\bar{N}_{(\lambda)}\right)|\Lambda(\nu_X,\nu_Y)|^2 \\ &+ |\Lambda(2\nu_X,2\nu_Y)|^2 \\ &+ \Lambda(2\nu_X,2\nu_Y)\left[\Lambda^*(\nu_X,\nu_Y)\right]^2 + \Lambda^*(2\nu_X,2\nu_Y)\left[\Lambda(\nu_X,\nu_Y)\right]^2 \\ &+ |\Lambda(\nu_X,\nu_Y)!^4 \, . \end{aligned} \qquad \text{(A-5)}$$

REFERENCES

1. L. Mandel, Proc. Phys. Soc. 72, 1037 (1958).
2. L. Mandel, Proc. Phys. Soc. 74 , 233 (1959).
3. W.E. Lamb, Jr., and M.O. Scully, "The Photoelectric Effect Without Photons", in Polarization, Matiere et Rayonnement (Societe Francaise de Physique, Paris) Presses Universitaires de France (1969), pp.363-369.
4. A. Papoulis, Probability, Random Variables, and Stochastic Processes, McGraw-Hill Book Co., New York, N.Y. (1965) p. 548.
5. A. Labeyrie, Astron. & Astrophys. 6, 85 (1970).
6. J.F. Walkup, Limitations in Interferometric Measurements and Image Restoration at Low Light Levels, Ph.D. Dissertation, Department of Electrical Engineering, Stanford University, July 1971.
7. J.J. Burke, "Estimating Objects from their Blurred and Grainy Images", Proceedings of the 1975 International Optical Computing Conference, (IEEE Catalog No. 75 CH0941-5C), Washington, D.C., April 1975, pp.48-51.
8. D. Fried, J. Opt. Soc. Am. 56, 1372 (1966).
9. R. Hugnagel, Appl. Opt. 10, 2547 (1971).

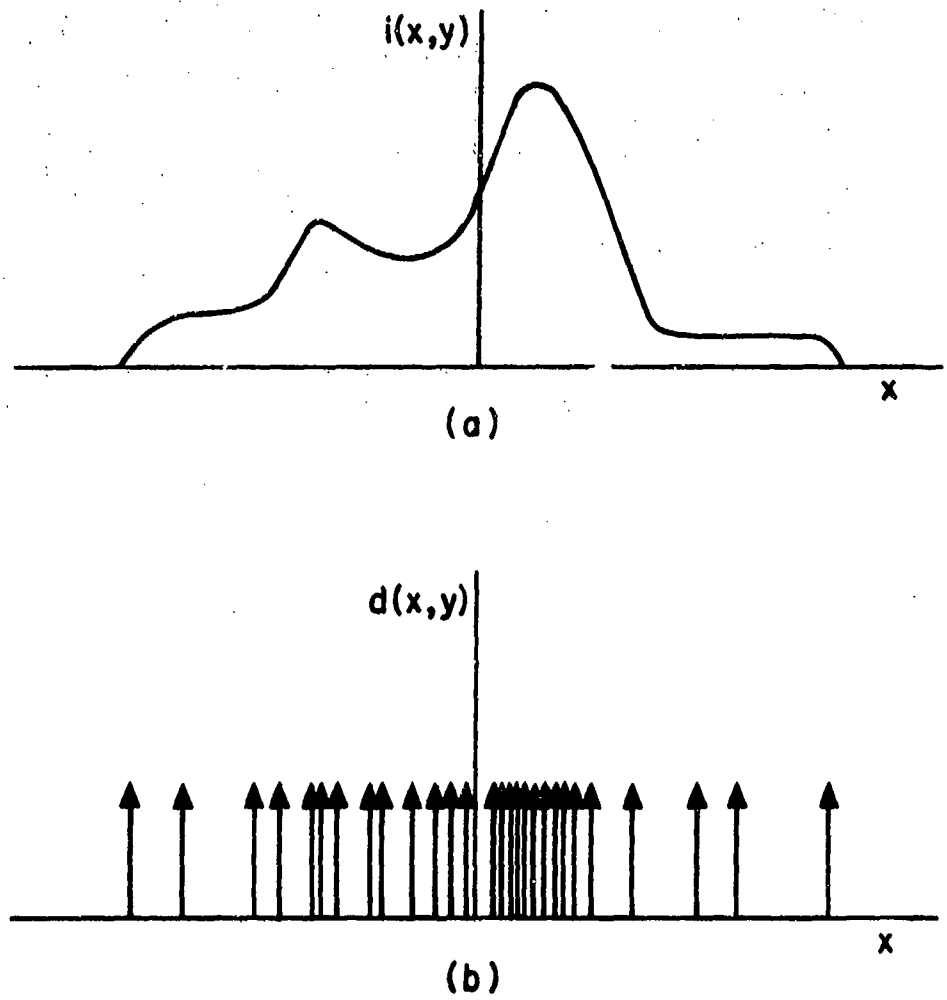

1. Model of photon-limited imagery: (a) classical intensity incident on detector; (b) resulting detected image.

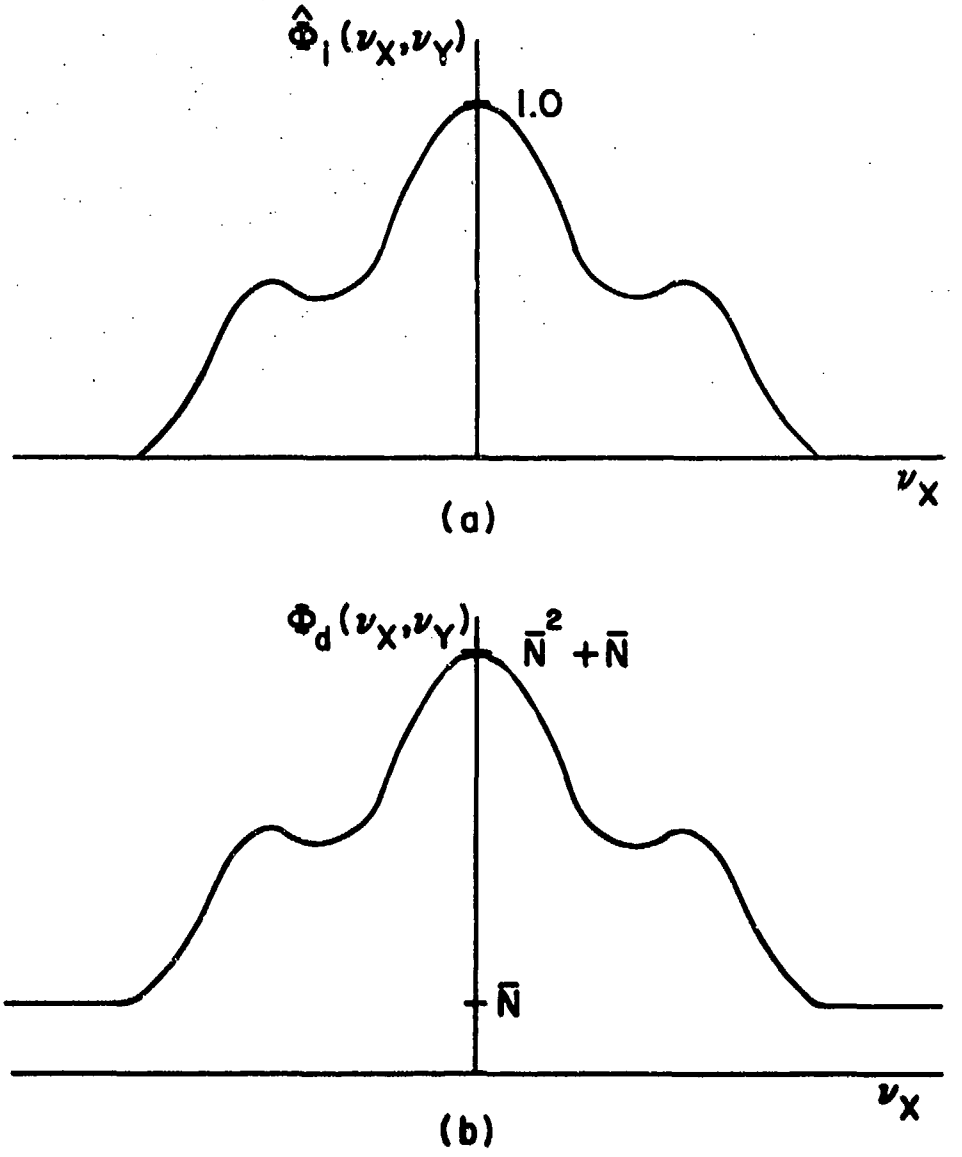

2. Relation between (a) normalized spectral density of the classical intensity distribution, and (b) spectral density of the detected image.

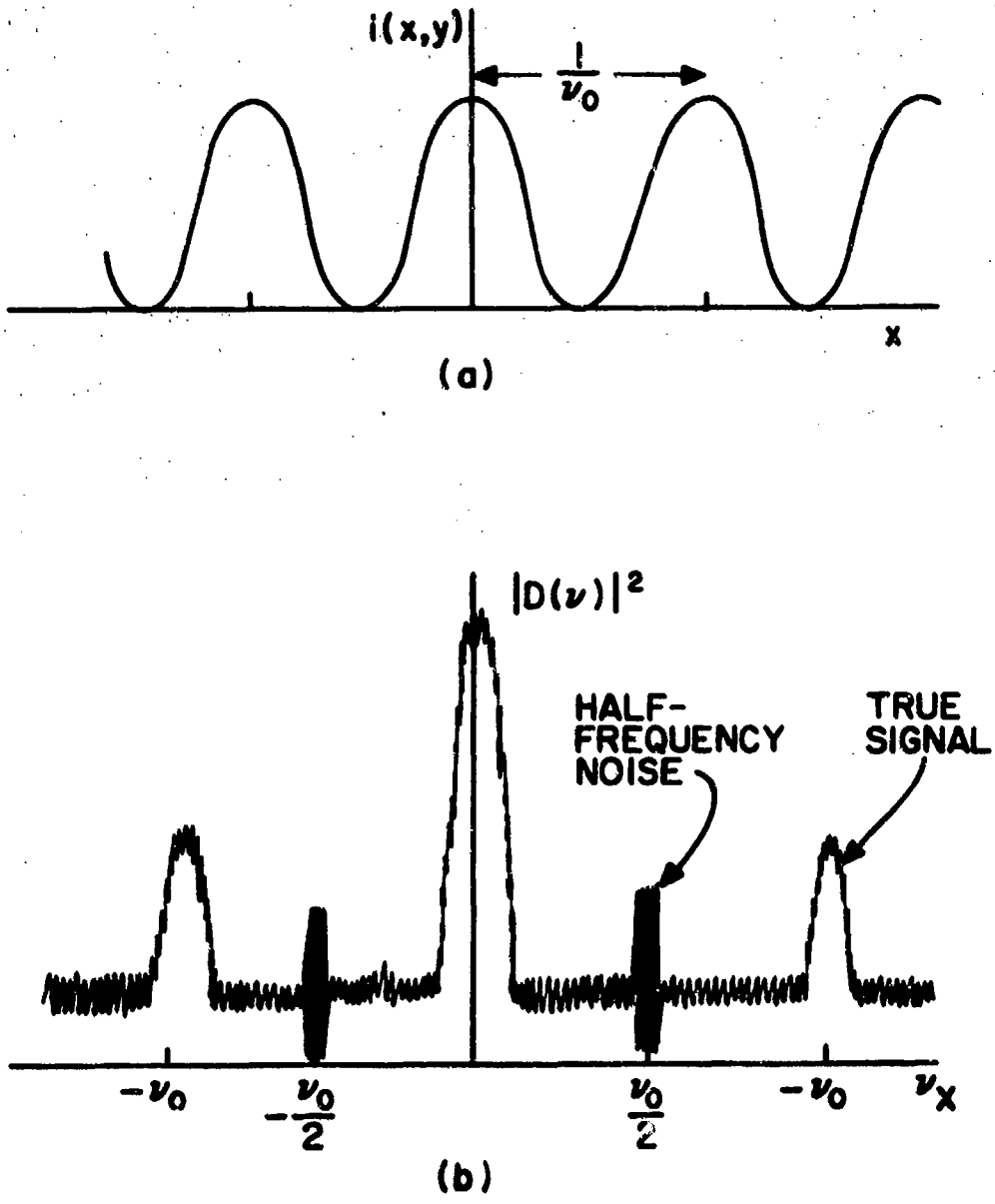

3. Single image estimate of spectral density illustrating "half-frequency" noise. (a) sinusoidal fringe of classical intensity; (b) single-image estimate of the spectral density of that intensity distribution.

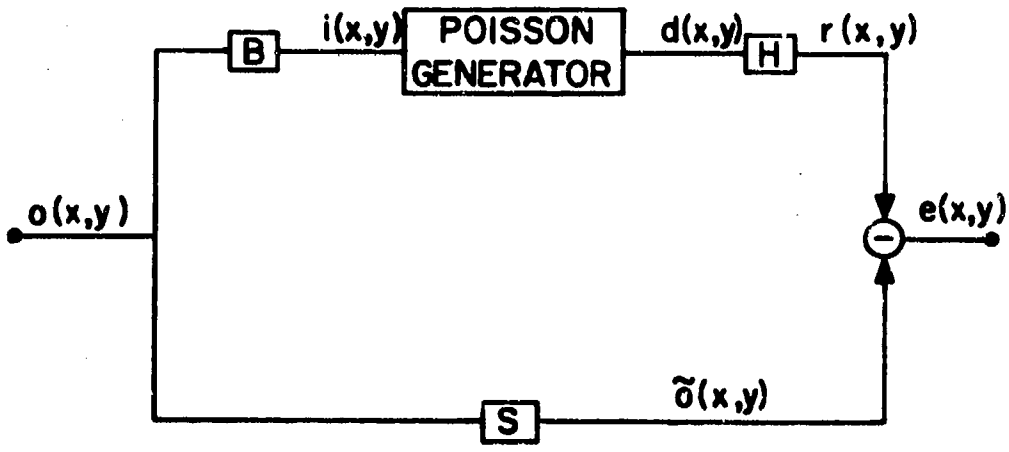

4. Block diagram for least-mean-square-error restoration.

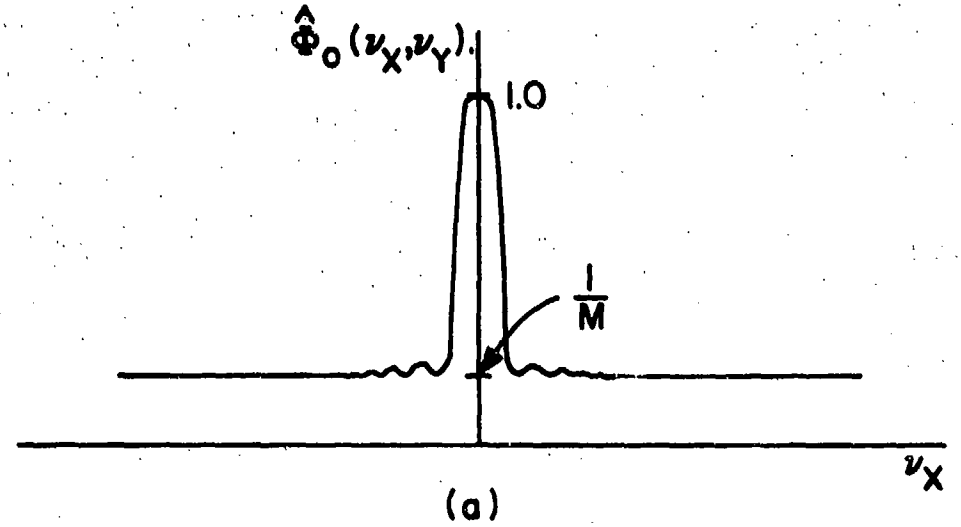

(a)

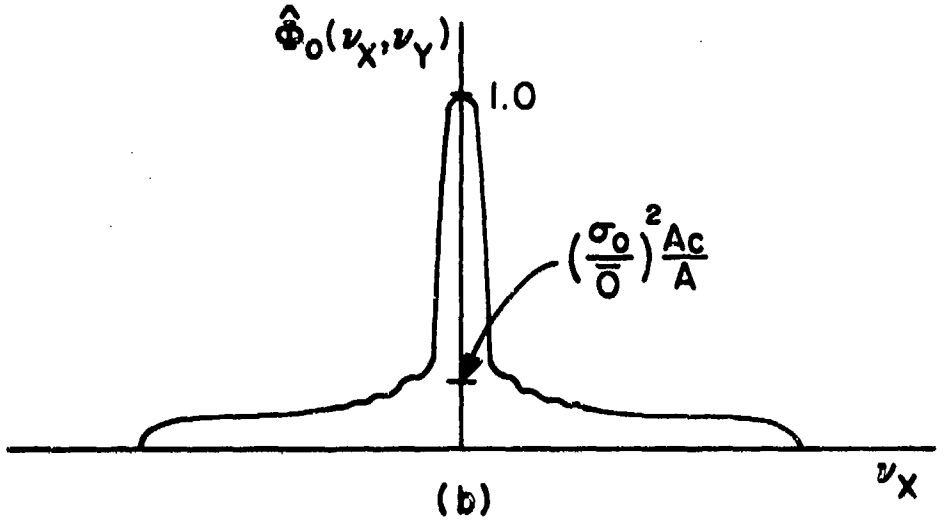

(b)

5. Normalized spectral densities for two object models: (a) M independent point sources, and (b) stationary object over a finite region.

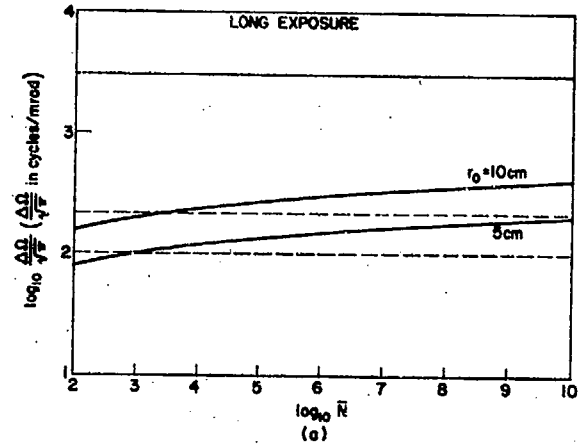

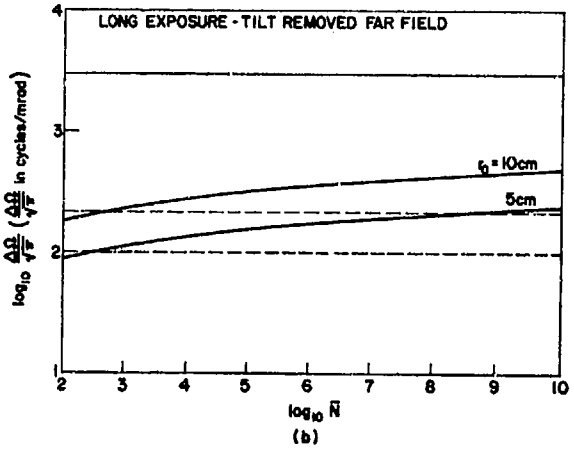

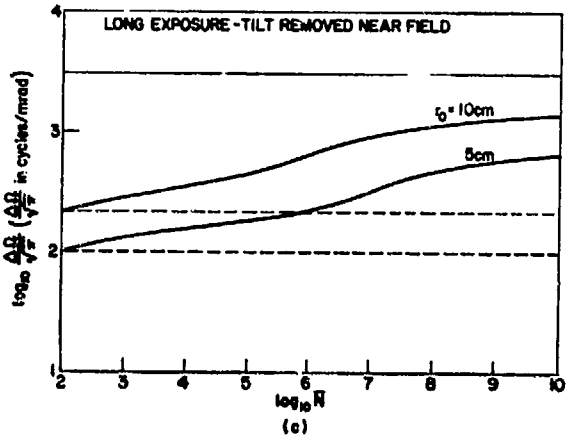

6. Maximum restorable frequency $\Delta\Omega/\sqrt{\pi}$ vs. $\bar{N}$ for r_o = 5 cm and 10 cm, D = 152 cm and $\bar{\lambda} = 5\times10^{-5}$ cm; (a) long exposure, no tilt removal, (b) long exposure, tilt removed, far-field atmospheric propagation, (c) long exposure, tilt removed, near-field atmospheric propagation. The solid horizontal line represents the telescope cutoff frequency D/λ, while the dashed horizontal lines represent r_o/λ for the t\ values of r_o used here.

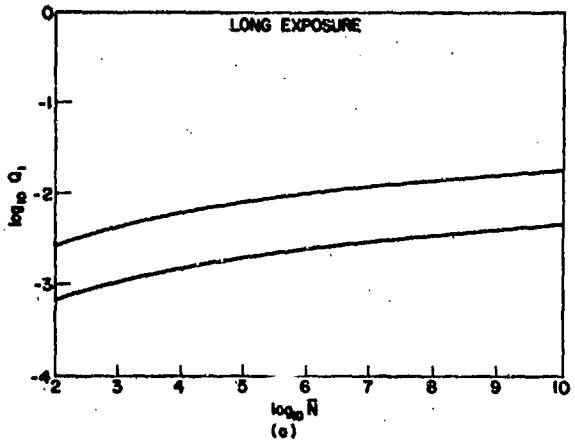

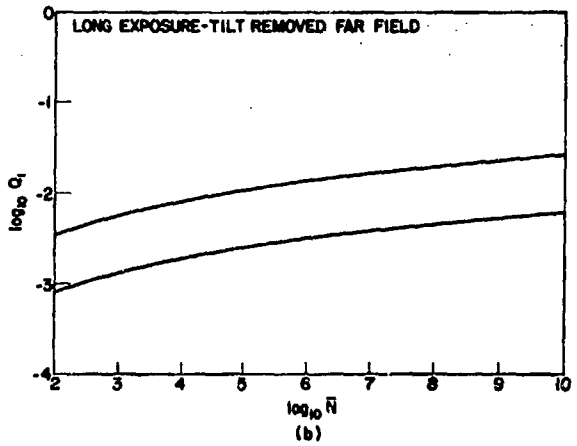

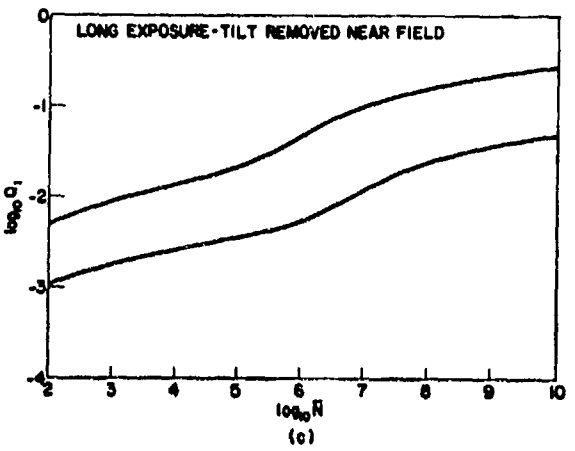

7. Quality parameter Q_1, for numbers identical with those of Fig. 6, parts (a),(b) and (c) corresponding to the same cases indicated there.